Journal of Power Sources 196 (2011) 1632–1638

Contents lists available at ScienceDirect

Journal of Power Sources

journal homepage: www.elsevier.com/locate/jpowsour

Enhanced performance of dye-sensitized solar cell with thermally-treated TiN in its TiO_2 film prepared at low temperature

Chuan-Pei Lee [a], Lu-Yin Lin [a], Keng-Wei Tsai [a], R. Vittal [a], Kuo-Chuan Ho [a,b,*]

[a] Department of Chemical Engineering, National Taiwan University, Taipei 10617, Taiwan
[b] Institute of Polymer Science and Engineering, National Taiwan University, Taipei 10617, Taiwan

ARTICLE INFO

Article history:
Received 21 February 2010
Accepted 14 September 2010
Available online 21 September 2010

Keywords:
Binder-free titanium dioxide
Dye-sensitized solar cell
Electron lifetime
Low temperature process
Thermally-treated titanium nitride

ABSTRACT

Various weight percentages of titanium nitride (TiN) and thermally-treated titanium nitride (tt-TiN) are incorporated into the binder-free TiO_2 films, prepared at low temperature (LT, 120 °C), and the corresponding dye-sensitized solar cells (DSSCs) are made. Effects of their incorporation on the photovoltaics of the DSSCs are studied. With the incorporation of 0.125 wt% of TiN in a TiO_2 film of only 5.5 μm-thickness, the corresponding solar-to-electricity conversion efficiency (η) has reached to 3.40% from 2.38% of a cell with a bare TiO_2 film of same thickness; this increase in efficiency is attributed to the higher electron conductivity and longer electron life time in the TiO_2 film with TiN. Incorporation of 1.0 wt% of tt-TiN into the TiO_2 film has further improved the conversion efficiency to 3.77%; this further enhancement in the efficiency is attributed to the partial conversion of TiN into TiO_2 due to the thermal treatment (450 °C). X-ray diffraction (XRD) and scanning electron microscopy (SEM) are used to study the partial conversion of TiN into TiO_2. Other explanations are supported by the data of UV-absorption spectra, electrochemical impedance spectroscopy (EIS), and laser-induced photo-voltage transients.

1. Introduction

Flexible dye-sensitized solar cells (DSSCs) are handy, convenient for transportation and can be used in complex environments. Cost-effective production of DSSCs can be achieved by using roll-to-roll printing process for electrode fabrication; this is possible with flexible DSSCs. It has been reported that the cell efficiency (η) increases with the increase of TiO_2-annealing temperature and becomes saturated at 400–500 °C; this was due to enhanced electron life time and increased electron diffusion coefficient for the excited electron in TiO_2 matrix [1,2]. High-temperature sintering cannot be applied to prepare TiO_2 film, because the substrate material is usually plastic. Organic binder is not suitable for preparing TiO_2 paste, as it cannot be removed at low temperatures. Without sintering at high temperature and without an organic binder, the interconnection between TiO_2 particles would be poor and would result in poor performance of the cell. Currently, research work is focused on the development of flexible dye-sensitized solar cells (DSSCs) based on nanocrystalline TiO_2 electrodes [3–7]. It is generally accepted that methods for the fabrication of DSSCs at low-temperature should solve two major problems, i.e., the incomplete necking of the TiO_2 particles and the removal of the residual organics within the TiO_2 film [6,8]. These problems affect electron transport and electron lifetime in the TiO_2 film, and consequently the cell performance. Recently, some reports have shown that incorporation of carbon nanotubes (CNTs) in TiO_2 films can provide efficient electron transfer through the films [9–12]. Meanwhile, some efforts have been made to develop methods compatible with plastic substrates, and the overall conversion efficiency reached 6.4% with a 10 μm thick TiO_2 film prepared with a binder-free TiO_2 paste [13,14].

Titanium nitride (TiN) is an extremely hard, conducting ceramic material, often used as a coating material for metal components to improve their surface properties [15–21]. TiN possesses very good conductivity [22] and it is biocompatible as well [23]. However, the literature on the use of TiN has been limited to its use in supercapacitors [24], as a substrate for electro-deposition of metals such as Pt, Cu, Ag or Zn [25–27], as a sensitive film for pH sensor [28], for deactivation of marine bacteria [29] and as a thin film on electrode for electro-analysis [30]. Platinized TiN is shown to be very good catalyst for the electrochemical oxidation of methanol [31].

Considering these features of TiN, we have incorporated various weight percentages of TiN and thermally-treated TiN (tt-TiN) into the low temperature (LT)-prepared TiO_2 films of only about 5.5 μm thickness, and studied the corresponding effects on the photovoltaics of pertinent dye-sensitized solar cells (DSSCs). Incorporation of TiN and thermally-treated TiN (tt-TiN) in TiO_2 photoanode and investigation of the pertinent effects on the pho-

* Corresponding author at: Department of Chemical Engineering, National Taiwan University, Taipei 10617, Taiwan. Tel.: +886 2 2366 0739; fax: +886 2 2362 3040.
E-mail address: kcho@ntu.edu.tw (K.-C. Ho).

0378-7753/$ – see front matter © 2010 Elsevier B.V. All rights reserved.
doi:10.1016/j.jpowsour.2010.09.022

tovoltaic parameters of the DSSCs is the essential novel aspect of this report. It is a proof of concept that TiN or thermally treated TiN (tt-TiN) as a conducting material in the photoanode of a DSSC can show beneficial effect in terms of its increased cell efficiency.

2. Experimental

Lithium iodide (LiI, analytical grade), and iodine (I_2, analytical grade) were obtained from Merck. N-methylbenzimidazole (NMBI, 99%), tetrabutylammonium iodide (TBAI, 98%), and tert-butyl alcohol (tBA, 96%) were obtained from Acros. Ti(IV) tetraisopropoxide (TTIP, >98%), acetonitrile (ACN, 99.99%), acetylacetone (AA, 99.5%), ethanol (99.5%), neutral cleaner, and isopropyl alcohol (IPA, 99.5%) were obtained from Aldrich.

Commercial titanium dioxide (P25, Degussa, 1.0 g) was added into a 6 ml-solution of tBA and DI-water (volume ratio: 2/1) and the contents were thoroughly mixed. The mixture was stirred for 5 days, and the binder-free TiO_2 paste was thus obtained. In a parallel process, various amounts of titanium nitride (TiN, Wako, 50 nm-sized) or thermally treated TiN (tt-TiN) were mixed with TiO_2 powders, and the corresponding pastes were prepared using the same processes mentioned above. The tt-TiN nanoparticles were obtained by placing TiN in an oven at 450 °C for 30 min. Crystal phases of tt-TiN were verified by X-ray diffraction (XRD, MO3XHF, MAC). The morphologies of LT-fabricated TiO_2 films with and without TiN or tt-TiN were observed from the images of scanning electron microscopy (SEM, LEO 1530, LEO Electron Microscopy). Film thickness was obtained using a surface profilometer (Sloan Dektak 3030).

Indium-doped SnO_2 conducting glass (ITO, 7 Ω sq.$^{-1}$, Ritek Corporation, Hsinchu, Taiwan) was first cleaned with a neutral cleaner, and then washed with DI-water, acetone, and IPA, sequentially. The conducting surface of the ITO was treated with a solution of TTIP (0.028 g) in ethanol (10 ml) for obtaining a good mechanical contact between the conducting glass and TiO_2 film, with and without TiN or tt-TiN, as well as for isolating the conducting glass surface from the electrolyte. A 5.5 μm-thick film of TiO_2 containing TiN or tt-TiN was coated by doctor blade method onto the treated conducting glass. The TiO_2/TiN (or tt-TiN) film was gradually heated to 120 °C in an oxygen atmosphere, and subsequently dried at that temperature for 1 h; it is because of this step that the fabrication of the DSSC is mentioned to be a low-temperature fabrication, as against the usual practice of sintering the TiO_2 film at 450 °C. After heating at 120 °C and cooling to 80 °C, the TiO_2/TiN (or tt-TiN) electrode was immersed in a 3×10^{-4} M solution of N719 (Solaronix S.A., Aubonne, Switzerland) in acetonitrile and tert-butyl alcohol (volume ratio of 1:1), at 55 °C for 1 h. The thus prepared TiO_2/TiN (or tt-TiN) electrode was coupled with a platinum-sputtered conducting glass electrode (ITO-Pt). The electrodes were separated by a 25 μm-thick Surlyn® (SX1170-25, Solaronix S.A., Aubonne, Switzerland) and sealed together by heating.

A mixture of 0.4 M LiI, 0.4 M TBAI, 0.04 M I_2, and 0.3 M NMBI in 3-methoxypropionitrile (MPN, Fluka)/ACN (volume ratio of 1:1) was used as the electrolyte. The electrolyte was injected into the gap between the electrodes through a hole by capillarity; the electrolyte-injecting hole was previously made in the counter electrode with a drilling machine. The hole was sealed with hot-melt glue after the electrolyte injection.

The surface of the DSSC was covered with a mask to control the illuminated area (0.237 cm^2) and thereby to obtain the photovoltaic parameters accurately. The cell was illuminated by a class A quality solar simulator (PEC-L11, AM1.5G, Peccell Technologies Inc., Japan) and the incident light intensity (100 mW cm^{-2}) was calibrated with a standard Si Cell (PECSI01, Peccell Technologies Inc., Japan). The photoelectrochemical characteristics of the DSSCs were recorded with a potentiostat/galvanostat (PGSTAT 30, Autolab, Eco-Chemie, the Netherlands). The set of equipments mentioned here was shown in our recent report [32].

UV–visible spectrophotometer (V-570, Jasco, Japan) was used to obtain absorption spectra of the dyes; for this the dye was dissolved from the TiO_2/TiN (or tt-TiN) film into 0.1 M $NaOH_{(aq)}$ and the solution was used for obtaining the spectra. Electrochemical impedance spectra (EIS) were obtained by the above-mentioned potentiostat/galvanostat equipped with an FRA2 module, under a constant light illumination of 100 mW cm^{-2}. The frequency range explored was 10 mHz to 65 kHz. The applied bias voltage was set at the open-circuit voltage of the DSSC, between the ITO-Pt counter electrode and the FTO-TiO_2-dye working electrode, starting from the short-circuit condition; the corresponding ac amplitude was 10 mV. The impedance spectra were analyzed using an equivalent circuit model [33,34]. The photovoltage transients of the assembled devices were recorded with a digital oscilloscope (model LT322, LeCroy, USA). Pulsed laser excitation was applied by a frequency-doubled Q-switched Nd:YAG laser (model Quanta-Ray GCR-3-10, Spectra-Physics laser) with a 2 Hz repetition rate at 532 nm, and a 7 ns pulse width at half-height. The average electron lifetime could approximately be estimated by fitting a decay of the open-circuit voltage transient with $\exp(-t\,\tau_e^{-1})$, where t is the time and τ_e is an average time constant before recombination.

3. Results and discussion

TiN is a conducting ceramic material with high electrical and thermal conductivity and considerable resistance to thermal shocks [15–31]. Considering these properties of TiN, we have incorporated it into TiO_2 films prepared at low-temperature (LT), and studied its influence on the photovoltaics of the respective DSSCs. The color of TiN nanoparticles is black, but the black powder turns into gray to the naked eye when sintered at 450 °C. The color change indicates a change in the chemical composition of the TiN nanoparticles, most likely an oxide formation, which indeed is established to be the partial formation of TiO_2 through XRD analysis. Fig. 1 shows the XRD spectra of TiN powder before and after its sintering. The thermally-treated TiN (tt-TiN) shows obvious peaks corresponding to (1 0 1) and (1 1 0) of the TiO_2 structure, namely, the anatase and rutile crystal phases, respectively. The partially derived TiO_2 in the tt-TiN can provide anchorage for additional adsorption of dye molecules. The tt-TiN is also expected to enhance the electron transport in the LT-fabricated TiO_2 film, owing to its TiN content (see Fig. 1) which is a better conductor than TiO_2.

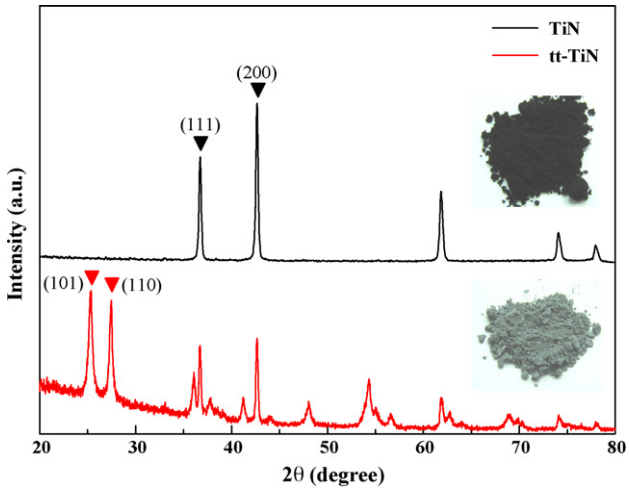

Fig. 1. XRD patterns of TiN before and after sintering at 450 °C.

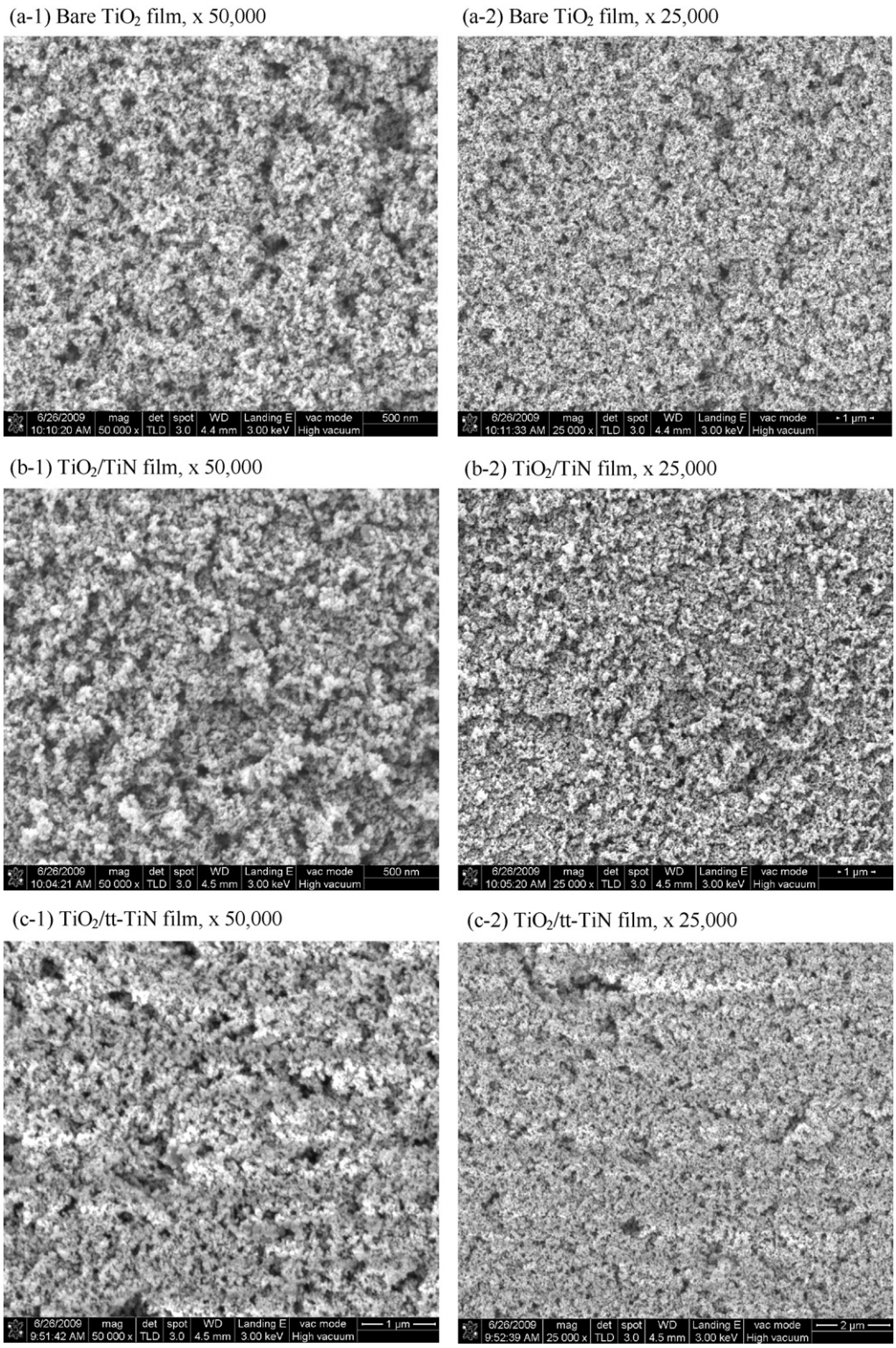

Fig. 2. SEM images of LT-prepared TiO_2 films without and with the addition of TiN or tt-TiN, obtained both at low and higher magnifications.

Fig. 2 shows scanning electron microscopic (SEM) images of LT-fabricated TiO_2 films, which were dried at 120 °C and formed from a binder-free paste without or with the addition of TiN or tt-TiN. For the binder-free paste, the inter-particle connection of nanocrystalline TiO_2 (necking reaction) is assumed to occur through the dehydration of hydrogen-bonded network of TiO_2 nanoparticles at low temperatures of 120–150 °C, in which the TiO_2 particles were surrounded by water molecules and their surfaces were covered with hydroxyl groups before heating at these temperatures [13]. Besides this, we propose for our present situation that small TiO_2 particles (P25, 20–25 nm) would surround relatively large TiN particles (~50 nm), in which the small TiO_2 particles get their own necking as proposed in [13]; these TiN particles, surrounded by the small TiO_2 particles, thus find necking with other TiO_2 particles in the bulk of the TiO_2 film. The entire mechanism including that from [13] is shown in Scheme 1. In other words the small TiO_2 particles

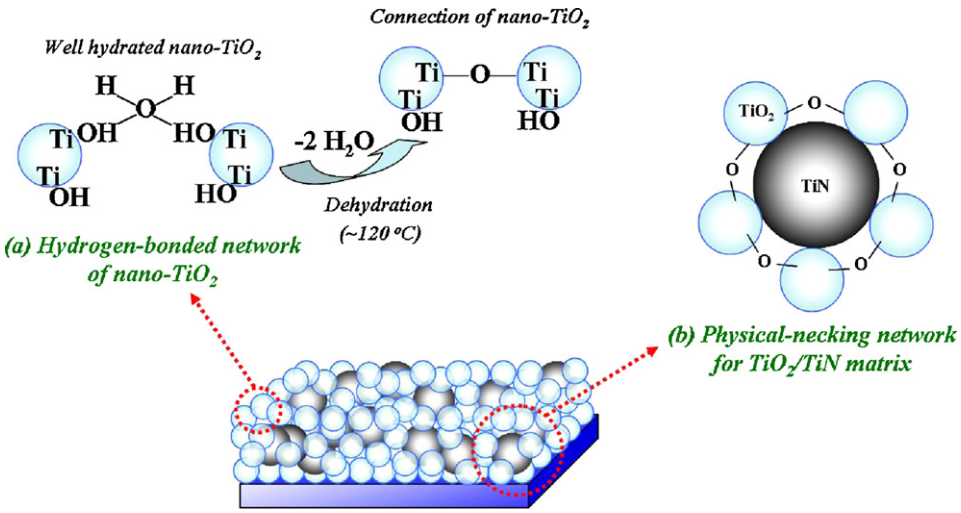

Scheme 1. A mechanism for inter-particle connection of (a) TiO_2 particles in a TiO_2 film prepared at low temperature and of (b) TiN particles with other bulk TiO_2 particles in the TiO_2 film.

act as physical-linkers to connect large TiN particles with the bulk TiO_2 particles in the TiO_2 film. In consistency with these explanations, the SEM images in Fig. 2 show that the LT-prepared films are uniform, mesoporous, and crack-free. The SEM images at higher magnification show that the nanoparticles are well interconnected.

The current–voltage (*I–V*) characteristics of DSSCs with different weight percentages of TiN in their LT-prepared TiO_2 films were measured under an illumination of 100 mW cm^{-2}. The *I–V* characteristics are shown in Fig. 3(a) and the corresponding photovoltaic parameters are listed in Table 1. The open-circuit voltage (V_{OC}), fill factor (*FF*), and short-circuit current density (J_{SC}) of the DSSC with bare TiO_2 electrode are 611 mV, 0.67, and 5.77 mA cm^{-2}, respectively, and the corresponding overall power conversion efficiency (η) is 2.38%. It can be seen in the table that the overall power conversion efficiencies are higher for DSSCs with the additions of 0.0625–0.5 wt% of TiN, than that for DSSC without any addition of it, due to substantial increases of V_{OC}, J_{SC}, and *FF* for the improved cells, except the case of 0.5% of TiN where the J_{SC} shows a relative decrease. Fig. 4a-1–4 shows the behavior of each individual photovoltaic parameter as a function of TiN content in the TiO_2 films. Table 1 shows that the best performance was obtained when the TiO_2 matrix contained 0.125 wt% TiN, with the values of 660 mV, 0.74, 6.91 mA cm^{-2}, and 3.4% for V_{OC}, *FF*, J_{SC}, and η, respectively. It can also be seen in Table 1 that the overall power conversion efficiencies are higher for DSSCs with the additions of 0.125–2.0 wt% of tt-TiN, than that without any addition of it, attributable to substantial increases of V_{OC}, J_{SC}, and *FF* for the improved cells, except the case of 2.0 wt% of tt-TiN where the J_{SC} shows a relative decrease. Fig. 4b-1–4 shows the behavior of each individual photovoltaic parameter as a function of tt-TiN content in the TiO_2 films.

Table 1
Photovoltaic parameters of DSSCs with various weight percentages of TiN and tt-TiN in their LT-prepared TiO_2 films.

Photoanode	V_{OC} (mV)	J_{SC} (mA cm^{-2})	η (%)	*FF*
Bare TiO_2	611	5.77	2.38	0.67
0.0625 wt% TiN	658	5.94	2.77	0.71
0.125 wt% TiN	660	6.91	3.40	0.74
0.25 wt% TiN	663	5.98	2.97	0.75
0.5 wt% TiN	648	5.60	2.80	0.77
0.125 wt% tt-TiN	617	6.67	2.80	0.68
0.25 wt% tt-TiN	646	6.85	3.16	0.71
0.5 wt% tt-TiN	637	7.33	3.44	0.74
1.0 wt% tt-TiN	640	8.09	3.77	0.73
2.0 wt% tt-TiN	629	5.39	2.45	0.72

Fig. 5 shows the UV–visible spectra of dyes desorbed from the bare TiO_2 film, the TiO_2 film with 0.125 wt% TiN, and the film with 1.0 wt% of tt-TiN. The spectra clearly shows that the dye-adsorption is lesser for the LT-prepared TiO_2 films both with 0.125 wt% of TiN and with 1.0 wt% of tt-TiN, than that for the bare TiO_2 film; the decrease in dye adsorption in the case of TiN or tt-TiN addition is

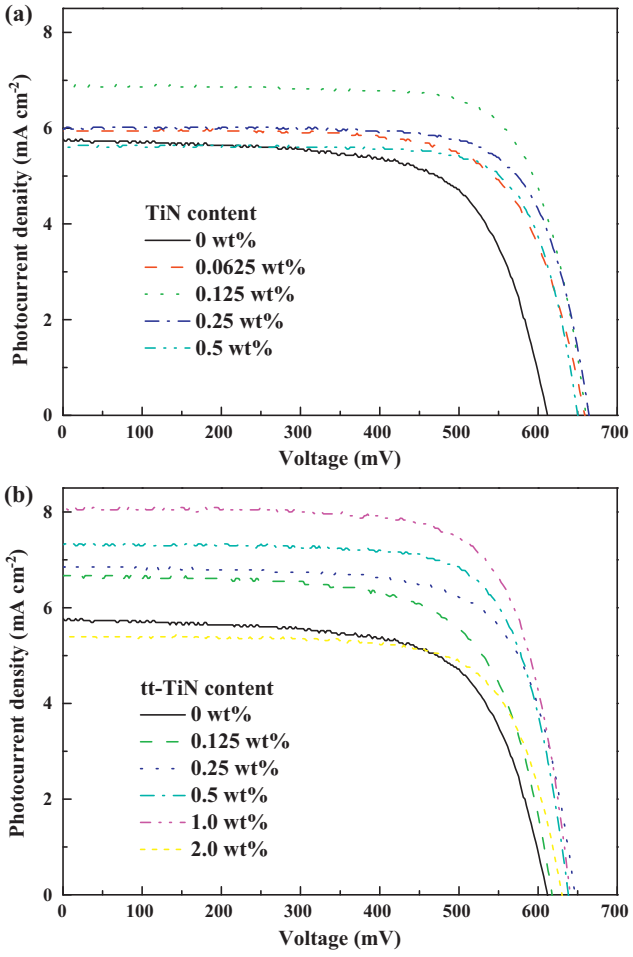

Fig. 3. Photocurrent–voltage characteristics of DSSCs with various weight percentages of TiN and tt-TiN in their LT-fabricated TiO_2 films, measured at 100 mW cm^{-2}.

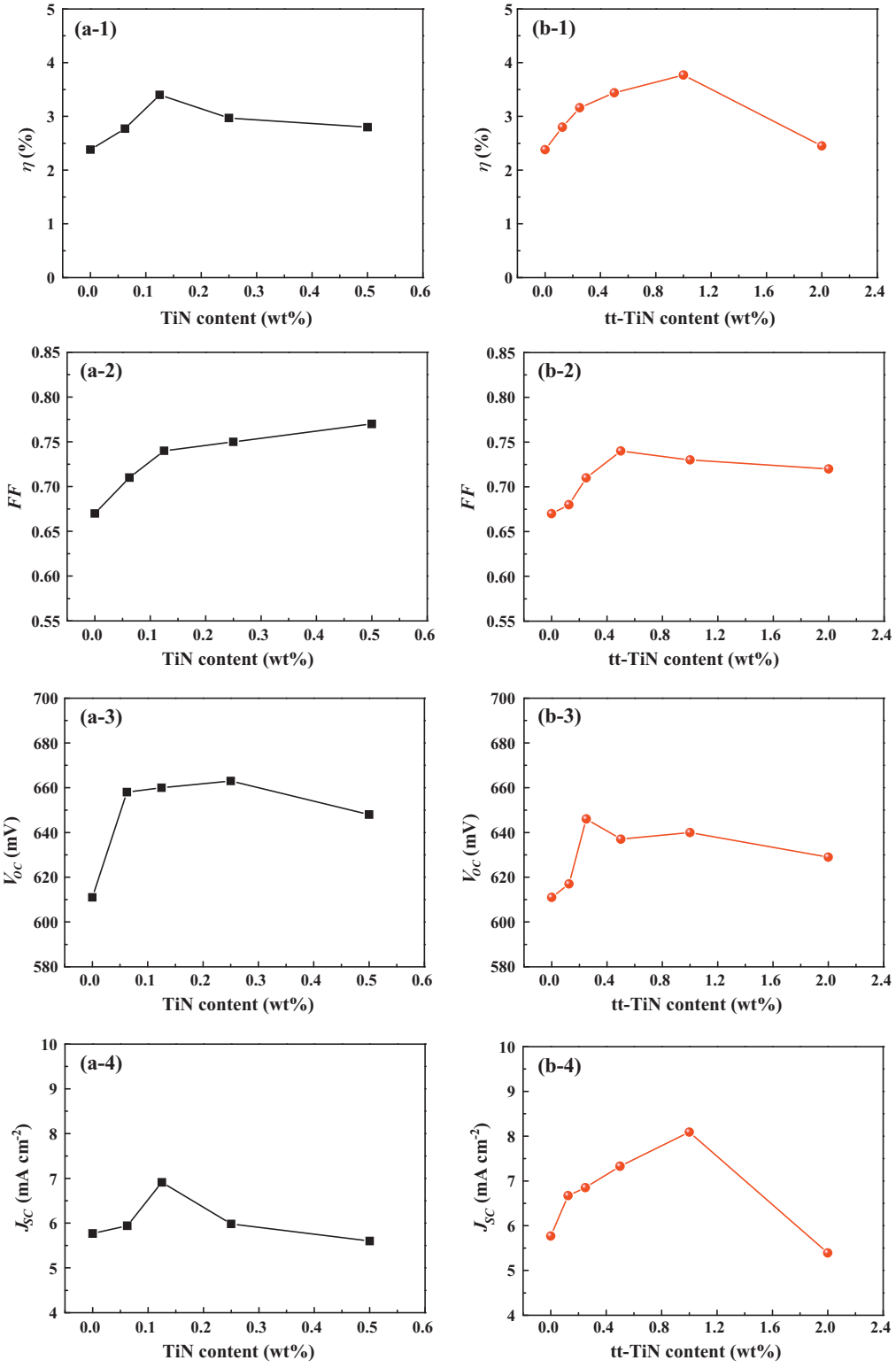

Fig. 4. Behavior of each photovoltaic parameter (η, *FF*, V_{OC}, and J_{SC}) as a function of TiN content in the TiO_2 film (a-1–4), and as a function of tt-TiN content in the TiO_2 film (b-1–4).

due to the decreased TiO_2 surface area available for dye-loading in the presence of it. The decrease in J_{SC} with 0.5 wt% of TiN and with 2.0 wt% of tt-TiN, with reference to that with the bare TiO_2 film is in consistency with this phenomenon, because decreased dye-loading causes decreased J_{SC}. Besides, excessive content of TiN or tt-TiN would result in a needless dark film, which is unfavorable for dye molecules to harvest the sunlight. A logical question arises here as to why other additions of TiN or tt-TiN have not decreased J_{SC}'s for their DSSCs. This may be explained considering that the beneficial effect of conductivity has overcompensated the detrimental effect of reduced dye-adsorption with respect to J_{SC} in the case of small additions of TiN or tt-TiN to the TiO_2 films. Apparently the limits for these additions are 0.25 wt% for TiN and 1.0 wt% for tt-TiN, in order to increase the respective J_{SC}'s; the difference in these limits are

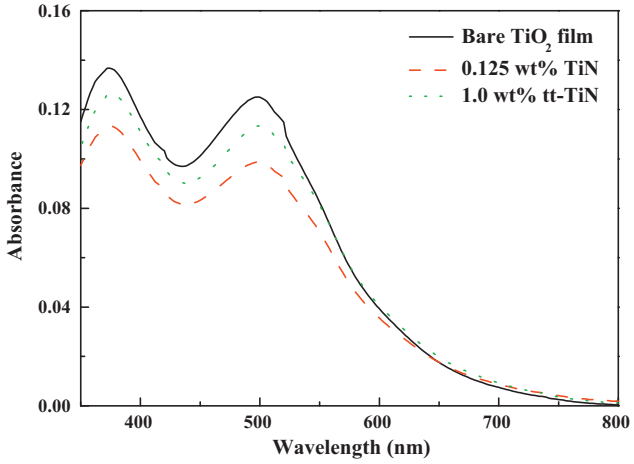

Fig. 5. UV–visible spectra of dyes, desorbed from bare TiO_2 film, TiO_2 film with 0.125 wt% of TiN, and TiO_2 film with 1.0 wt% of tt-TiN.

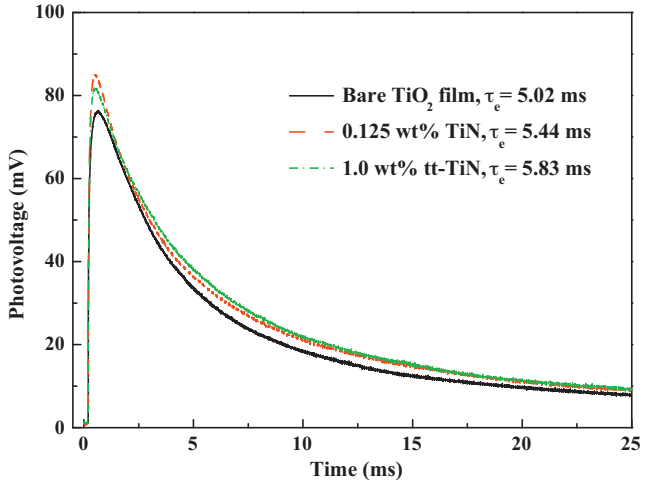

Fig. 7. Transient photovoltage measurements of DSSCs with bare TiO_2 film, TiO_2 film with 0.125 wt% of TiN, and TiO_2 film with 1.0 wt% of tt-TiN.

apparently due to the fact that the partially derived TiO_2 in tt-TiN can provide anchorage for additional adsorption of dye molecules and thereby contribute for increased J_{SC}. This explanation is also in consistency with the observation in Fig. 5, in which 1.0 wt% of tt-TiN shows higher loading of dye for its TiO_2 than 0.125 wt% of TiN for its TiO_2.

The best performance in the case of addition of tt-TiN can be noticed with the addition of 1.0 wt% tt-TiN, with the values of 640 mV, 0.73, 8.09 mA cm^{-2}, and 3.77% for V_{OC}, FF, J_{SC}, and η, respectively. The partially derived additional TiO_2 from the tt-TiN can provide additional anchorage for dye molecules, compared to the case of addition of TiN. This additional anchorage of dye-molecules has rendered a far higher J_{SC} for the DSSC with tt-TiN, than that for the DSSC with mere TiN; this increase in J_{SC} is the essential cause for the overall higher conversion efficiency of the DSSC with tt-TiN than that of the cell with TiN. Content of tt-TiN in excess 1.0 wt% of tt-TiN has resulted in a great decrease in its J_{SC}, due to an unfavorable dark film for the absorption of light, thereby exhibiting the lowest η for the corresponding cell.

Fig. 6 shows electrochemical impedance spectra (EIS) of DSSCs with bare TiO_2 film, TiO_2 film with 0.125 wt% TiN, and TiO_2 film with 1.0 wt% of tt-TiN. The corresponding equivalent circuit is illustrated in the inset of the figure. In general, the EIS spectrum of a FTO/TiO_2/dye/electrolyte/Pt/ITO device shows three semicircles in

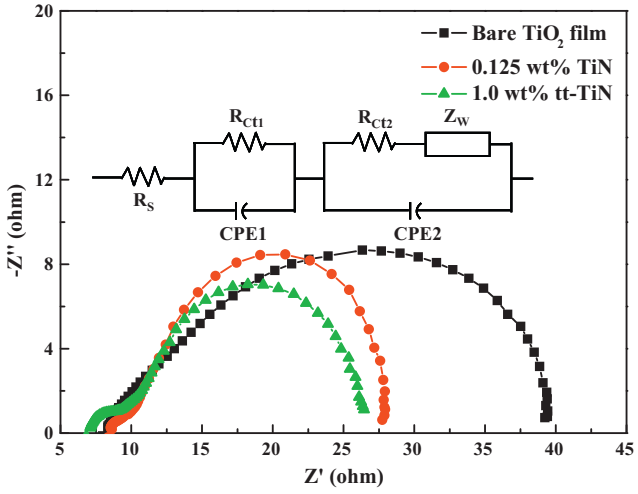

Fig. 6. EIS spectra of DSSCs with bare TiO_2 film, TiO_2 film with 0.125 wt% of TiN, and TiO_2 film with 1.0 wt% of tt-TiN, measured at 100 mW cm^{-2}.

the frequency range of 10 mHz to 65 kHz. The ohmic serial resistance (R_S) corresponds to the overall series resistance. The first and second semicircles correspond to the charge-transfer resistances at the counter electrode (R_{ct1}) and the TiO_2/dye/electrolyte interface (R_{ct2}), respectively. The Warburg diffusion process of I^-/I_3^- in the electrolyte (R_{diff}) is associated with the third semicircle. However, in our work the conventional diffusion resistance of the redox couple is apparently greatly overlapped by R_{ct2} due to a short length for I^- ion diffusion available with the thin spacer used (25 μm thick), and owing to the low viscosity of the solvents used in our electrolyte (viscosities of ACN and MPN are 0.37 cP and 1.60 cP, respectively). It can be seen that R_{ct2} decreases in the case of DSSCs with 0.125 wt% TiN and 1.0 wt% tt-TiN, the decrease being greater for the case of tt-TiN. The decreased interfacial resistance (R_{ct2}) is the reason for the higher FFs (Table 1) of the respective dye-sensitized solar cells (DSSCs), compared to that of the cell with a bare TiO_2 film (Table 1).

The average electron lifetimes (τ_e) in the TiO_2 films were also obtained by a laser-induced photo-voltage transient technique, and the data are shown in Fig. 7. The average electron lifetime can approximately be estimated by fitting a decay of the open-circuit voltage transient with $\exp(-t\,\tau_e^{-1})$, where t is the time and τ_e is an average time constant before recombination. The values of τ_e were found to be 5.02, 5.44 and 5.83 ms for the DSSCs with bare TiO_2 film, TiO_2 film with 0.125 wt% of TiN, and TiO_2 film with 1.0 wt% of tt-TiN, respectively. The values clearly show that the average electron lifetime in the TiO_2 films with 0.125 wt% of TiN or with 1.0 wt% of tt-TiN is much longer than that in the bare TiO_2 film. The results are in consistency with the higher J_{SC}'s observed for the cells with 0.125 wt% of TiN and 1.0 wt% of tt-TiN than that of the cell without any of them. The rutile content of TiO_2 in the case of tt-TiN (Fig. 1) could also contribute for the higher J_{SC} for the corresponding DSSC than that of the cell with TiN, because rutile TiO_2 can scatter the light better than anatase TiO_2. Longer electron lifetimes in TiO_2 films lead to reduced recombination reactions and thereby to increased V_{OC}'s, as is observed for the DSSCs with TiN and tt-TiN, with reference to that of the cell without any of them (Table 1).

Finally, it is to be noted that the DSSCs were fabricated using very thin TiO_2 films of about 5.5 μm each prepared at low temperature, and the pertinent efficiencies are thus low in general. The selection of such a thin film is intended to focus our study on the effects of additions of TiN and tt-TiN into the TiO_2 films on the photovoltaic parameters of the pertinent cells; such thin film is also intended to avoid needless dark films in our preliminary studies on DSSCs with LT-prepared TiO_2 films.

4. Conclusions

DSSCs with the additions of 0.125 wt% of TiN and 1.0 wt% of thermally treated TiN (tt-TiN) to their low-temperature prepared TiO_2 matrixes (5.5 μm thick) exhibited considerably higher solar-to-electricity conversion efficiencies (η) than the corresponding DSSC without these additions. The improved efficiencies were due to substantial increases in respective J_{SC}'s, V_{OC}'s, and *FF*s. DSSC with 1.0 wt% of tt-TiN exhibited higher J_{SC} and η than those of the cell with 0.125 wt% of TiN. Partial conversion of TiN into TiO_2 (XRD) rendered additional anchorage to the adsorption of dye molecules to the TiO_2 film (UV–visible spectra) and thereby enhanced J_{SC} and η for the DSSC with tt-TiN, with reference to the case of DSSC with TiN. Reduced interfacial charge transfer resistance at TiO_2/dye/electrolyte (EIS) is understood to be the reason for the increased *FF*, and longer electron lifetime in TiO_2 film (by transient photovoltage measurements) is seen as the reason for increased V_{OC} for both the DSSCs with TiN and tt-TiN, with reference to the case of DSSC without these additions.

Acknowledgements

This work was supported in part by the National Research Council of Taiwan under grant numbers NSC 96-2120-M-002-016, NSC 97-2120-M-002-012 and NSC 98-2120-M-002-003. Some of the instruments used in this study were made available through the financial support of the Academia Sinica, Nankang, Taipei, Taiwan.

References

[1] S. Nakade, M. Matsuda, S. Kambe, Y. Saito, T. Kitamura, T. Sakata, Y. Wada, H. Mori, S. Yanagida, J. Phys. Chem. B 106 (2002) 10004–10010.
[2] K.M. Lee, V. Suryanarayanan, K.C. Ho, Sol. Energy Mater. Sol. Cells 91 (2007) 1416–1420.
[3] F. Pichot, J.R. Pitts, B.A. Gregg, Langmuir 16 (2000) 5626–5630.
[4] D. Zhang, T. Yoshida, H. Minoura, Adv. Mater. 15 (2003) 814–817.
[5] T. Miyasaka, Y. Kijitori, J. Electrochem. Soc. 151 (2004) A1767–A1773.
[6] L.N. Lewis, J.L. Spivack, S. Gasaway, E.D. Williams, J.Y. Gui, V. Manivannan, O.P. Siclovan, Sol. Energy Mater. Sol. Cells 90 (2006) 1041–1051.
[7] X. Li, H. Lin, J. Li, N. Wang, C. Lin, L. Zhang, J. Photochem. Photobiol. A: Chem. 195 (2008) 247–253.
[8] C. Longo, A.F. Nogueira, M.A. DePaoli, H. Cachet, J. Phys. Chem. B 106 (2002) 5925–5930.
[9] S.R. Jang, R. Vittal, K.J. Kim, Langmuir 20 (2004) 9807–9810.
[10] S.L. Kim, S.R. Jang, R. Vittal, J. Lee, K.J. Kim, J. Appl. Electrochem. 36 (2006) 1433–1439.
[11] T.Y. Lee, P.S. Alegaonkar, J.B. Yoo, Thin Solid Films 515 (2007) 5131–5135.
[12] K.M. Lee, C.W. Hu, H.W. Chen, K.C. Ho, Sol. Energy Mater. Sol. Cells 92 (2008) 1628–1633.
[13] Y. Kijitori, M. Ikegami, T. Miyasaka, Chem. Lett. 36 (2007) 190–191.
[14] T. Miyasaka, M. Ikegami, Y. Kijitori, J. Electrochem. Soc. 154 (2007) A455–A461.
[15] W. Schintlmeister, O. Pacher, K. Pfaffinger, T. Raine, J. Electrochem. Soc. 123 (1976) 924–929.
[16] J.S. Cho, S.W. Nam, J.S. Chun, J. Mater. Sci. 17 (1982) 2495–2502.
[17] M. Li, S. Luo, C. Zeng, J. Shen, H. Lin, C. Cao, Corros. Sci. 46 (2004) 1369–1380.
[18] Y. Wang, D.O. Northwood, J. Power Source 165 (2007) 293–298.
[19] Y. Wang, D.O. Northwood, Int. J. Hydrogen Energy 32 (2007) 895–902.
[20] A.A.C. Recco, D. López, A.F. Bevilacqua, F. da Silva, A.P. Tschiptschin, Surf. Coat. Technol. 202 (2007) 993–997.
[21] S.T. Myung, M. Kumagai, R. Asaishi, Y.K. Sun, H. Yashiro, Electrochem. Commun. 10 (2008) 480–484.
[22] M. Wittmer, B. Studer, H. Melchior, J. Appl. Phys. 52 (1981) 5722–5726.
[23] T. Röstlund, P. Thomsen, L.M. Bjursten, L.E. Ericson, J. Biomed. Mater. Res. 24 (1990) 847–860.
[24] D. Choi, P.N. Kumta, J. Electrochem. Soc. 153 (2006) A2298–A2303.
[25] H. Cesiulis, M. Ziomek-Moroz, J. Appl. Electrochem. 30 (2000) 1261–1268.
[26] S.A.G. Evans, J.G. Terry, N.O.V. Plank, A.J. Walton, L.M. Keane, C.J. Campbell, P. Ghazal, J.S. Beattie, T.J. Su, J. Crain, A.R. Mount, Electrochem. Commun. 7 (2005) 125–129.
[27] E.E. Ferapontova, J.G. Terry, A.J. Walton, C.P. Mountford, J. Crain, J.A.H. Buck, P. Dickinson, C.J. Campbell, J.S. Beattie, P. Ghazal, P.A.R. Mount, Electrochem. Commun. 9 (2007) 303–309.
[28] Y. Wang, H. Yuan, X. Lu, Z. Zhou, D. Xiao, Electroanalysis 18 (2006) 1493–1498.
[29] T. Nakayama, H. Wake, K. Ozawa, H. Kodama, N. Nakamura, T. Matsunaga, Environ. Sci. Technol. 32 (1998) 798–801.
[30] C.N. Kirchner, K.H. Hallmeier, R. Szargan, T. Raschke, C. Radehaus, G. Wittstock, Electroanalysis 19 (2007) 1023–1031.
[31] O.T.M. Musthafa, S. Sampath, Chem. Commun. (2008) 67–69.
[32] C.P. Lee, K.M. Lee, P.Y. Chen, K.C. Ho, Sol. Energy Mater. Sol. Cells 93 (2009) 1411–1416.
[33] L. Han, N. Koide, Y. Chiba, T. Mitate, Appl. Phys. Lett. 84 (2004) 2433–2435.
[34] L. Han, N. Koide, Y. Chiba, A. Islam, T. Mitate, C. R. Chimie 9 (2006) 645–651.